



Western Michigan University
ScholarWorks at WMU

Master's Theses

Graduate College

12-2015

An Integrated Framework for Cardiac Sounds Diagnosis

Zichun Tong

Follow this and additional works at: https://scholarworks.wmich.edu/masters_theses



Part of the Computer Engineering Commons, and the Electrical and Computer Engineering Commons

Recommended Citation

Tong, Zichun, "An Integrated Framework for Cardiac Sounds Diagnosis" (2015). *Master's Theses*. 671.
https://scholarworks.wmich.edu/masters_theses/671

This Masters Thesis-Open Access is brought to you for free and open access by the Graduate College at ScholarWorks at WMU. It has been accepted for inclusion in Master's Theses by an authorized administrator of ScholarWorks at WMU. For more information, please contact wmu-scholarworks@wmich.edu.



AN INTEGRATED FRAMEWORK FOR CARDIAC SOUNDS DIAGNOSIS

by

Zichun Tong

A thesis submitted to the Graduate College
in partial fulfillment of the requirements
for a degree of Master of Science in Engineering
Electrical and Computer Engineering
Western Michigan University
December 2015

Thesis Committee:

Ikhlas Abdel-Qader, Ph.D., Chair

Raghe Gejji, Ph.D.

Azim Houshyar, Ph.D.

AN INTEGRATED FRAMEWORK FOR CARDIAC SOUNDS DIAGNOSIS

Zichun Tong, M.S.E.

Western Michigan University, 2015

The Phonocardiogram (PCG) signal contains valuable information about the cardiac condition and is a useful tool in recognizing dysfunction and heart failure. By analyzing the PCG, early detection and diagnosis of heart diseases can be accomplished since many pathological conditions of the cardiovascular system cause murmurs or abnormal heart sounds. This thesis presents an algorithm to classify normal and abnormal heart sound signals using PCG. The proposed analysis is based on a framework composed of several statistical signal analysis techniques such as wavelet based de-noising, energy-based segmentation, Hilbert-Huang transform based feature extraction, and Support Vector Machine based classification. The MATLAB test results using PCG recordings validate the model used in the proposed system with very high classification accuracy averaged at 90.5%.

© 2015 Zichun Tong

ACKNOWLEDGMENTS

First I would like to thank my advisor and committee chair Dr. Ikhlas Abdel-Qader for her experienced guidance and optimism encouragement. Her vision and creativeness has inspired this work. I am also indebted to Ikhlas for her endless patience, generous support, and experienced guidance.

I would also like to thank the members of my thesis committee: Dr. Raghe Gejji and Dr. Azim Houshyar for their time and their feedback on my work.

Additionally, I am fortunate to have many good friends around me at Kalamazoo. I would like to thank all of them for their great help in my life.

Finally, I would like to take this opportunity to thank my parents Benjun Tong and Xiaozhen Wang for their unconditional love and support. I would like to dedicate this thesis to them for their endless love.

Zichun Tong

TABLE OF CONTENTS

ACKNOWLEDGMENTS	ii
LIST OF TABLES	v
LIST OF FIGURES	vi
1. INTRODUCTION	1
1.1 Background	1
1.2 Literature Review	3
1.3 Scope and Objective	4
1.4 Thesis Organization	5
2. HEART AND HEART SOUNDS	7
2.1 Cardiac Physiology	7
2.2 Heart Sounds	8
2.3 Heart Murmurs	10
3. WAVELET BASED DENOSING OF HEART SOUND	13
3.1 Introduction to Wavelet Analysis	13
3.2 Wavelet Threshold De-noising	13

Table of Contents—Continued

3.3 Wavelet Based De-noising Experiment	16
4. SEGMENTATION OF HEART SOUND	19
4.1 Method	19
4.2 Results and Discussion	22
5. FEATURE EXTRACTION AND CLASSIFICATION	25
5.1 Introduction.....	25
5.2 Hilbert-Huang Transformation	25
5.3 Support Vector Machine	29
6. SIMULATIONS AND EXPERIMENT RESULTS	33
6.1 Heart Sound Analysis by HHT	33
6.2 Feature Extraction.....	37
6.3 Heart Sound Classification	38
7. CONCLUSIONS AND FUTURE WORK	40
BIBLIOGRAPHY	42

LIST OF TABLES

1. The result of heart sounds segmentation.....	24
2. The result of the classification of the test sets consisting of 21 cases	39
3. The percentage accuracy of the SVM classification.....	39

LIST OF FIGURES

1. Proportion of global deaths under the age 70 years (2012)	2
2. Flowchart of thesis work.....	6
3. The anatomy of the human heart	8
4. The sequence of cardiac cycle(PCG ECG and the pressure).....	9
5. Shapes of an innocent systolic ejection murmur.....	11
6. Shape of an ejection murmur	12
7. Pulmonary insufficiency in absence of pulmonary hypertension	12
8. The waveform of the test complex exponential signals.....	17
9. Result of the wavelet threshold de-noising experiment.....	18
10. The overlap between two adjacent sections.....	20
11. Detection of Single S1 S2 in normal heart sound	23
12. Detection of heart sound with Holo Systolic Murmur.....	23
13. Detection of heart sound with Systolic and Diastolic Murmurs	24
14. The block diagram to calculate the IMFs	27
15. Maximum-margin hyperplane and margins for an SVM trained with samples from two classes.....	30

List of Figures—Continued

16. The empirical mode decomposition of normal heart sound. (row1) Data,
 (row2-10) nine IMF components, (row11) the final residue components ...34
17. The empirical mode decomposition of abnormal heart sound. (row1) Data,
 (row2-10) nine IMF components, (row11) the final residue components ...35
18. Hilbert boundary spectrum of the normal heart sound36
19. Hilbert boundary spectrum of the abnormal heart sound.....36

CHAPTER I

INTRODUCTION

1.1 Background

Phonocardiography (PCG), tracing of sounds produced by digital stethoscope, is a tool that lead to invaluable information about the heart function and can be a great tool to identify abnormalities and heart disease early on. Meanwhile, cardiovascular disease (CVDs) become one of the leading risk factors for global mortality in modern society. Fig.1 shows the proportion of non-communicable diseases (NCDs) deaths under the age of 70 years. Cardiovascular diseases are the largest proportion of NCD deaths (37%), followed by cancers and chronic respiratory diseases. CVDs are the number 1 cause of death globally: more people die annually from CVDs than from any other cause[1].

However, the majority of people are not aware of having CVD because it is usually asymptomatic until the damaging effects (such as heart pain, stroke, renal dysfunction) are observed. People with cardiovascular disease or at high cardiovascular risk are in need for early detection methods and management tools to prevent the detriment from CVDs. Consequently, self-auscultation in daily life is an effective measure in CVDs prevention and treatment[2], which provides a measurement of one's heart condition and can help establish the diagnosis of CVDs and monitor the effects of medication taken.

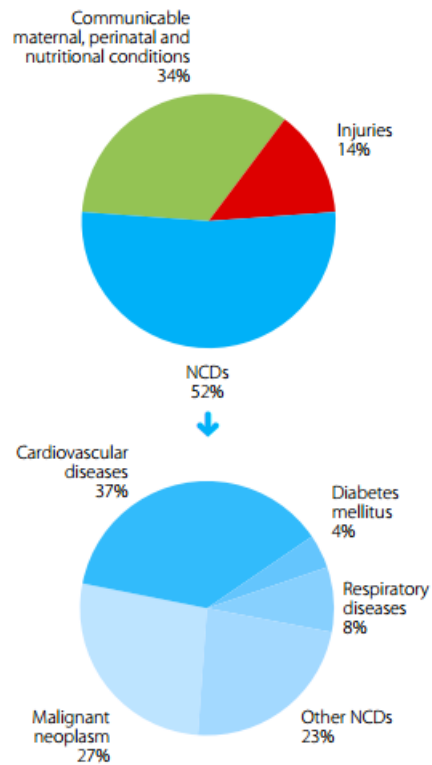


Figure 1. Proportion of global deaths under the age 70 years (2012) [1]

Heart sound signal is an important physiological signals of cardiovascular system, which contains important diagnostic information such as physiological and pathological messages. Normally, the cardiovascular diseases may be reflected in the heart sounds much earlier than in other signals [2]. The heart sounds signal has its own advantages such as convenience, low cost, and low maintenance needs that electrocardiogram signal (ECG) cannot replace. This makes heart auscultation become a basic detection method. However, the auscultation is susceptible by the physician's subjective, the auscultation accuracy is influenced by the experience of clinical staff. Moreover, a study showed that the most sensitive frequency range of the human ear was between 1000 and 3000 Hz [2], while the frequency components of heart sounds were most between 40 and 100Hz, some low frequency sounds that have

important diagnostic value cannot be distinguished. Therefore, there is a need for automated detection and consequently classification of heart sound signal.

The technology of PCG improves cardiovascular disease diagnosis because PCG can be stored and analyzed using specific algorithms to extract essential information [3]. This thesis is focused on phonocardiogram (PCG) analysis, signal source separation, and classification. Proper PCG analysis will allow acoustic visualization of the heart sound with precise timing and relative intensities. An intelligent system for PCG analysis can be composed from three stages or subsystems. The first stage is considered as a pre-process which purposed to eliminate noise and to perform a segmentation procedure. The second stage is to isolate the major heart sounds and feature extraction while the third process is to perform the identification of heart sounds and classify them.

1.2 Literature Review

With the rapid development in digital technology, a variety of methods are shifting attention to the analysis of heart sounds in recent years. Earlier studies such as Travel [3] and Leatham [2] identified the temporal and spectral characters of heart sounds and specifically murmurs and presented an association link between the characters and the underlying diseases.

In [4], the short-time Fourier Transform was used to construct a transfer function and a coherence function relating to cardiac vibration while in [5], Liang

provided a method based on discrete wavelet decomposition and reconstruction to produce envelopes of approximations and details to extract features from PCG. Also, Popov in [6] used Chirplets to extract the components of aortic and pulmonary signals from in heart sound recordings in animals. Their results ended in use widely for the measurement of pulmonary artery pressure. Recently, Syed [7] provides a framework for the analysis of heart sound signals that compares a large number of different previous analysis methods and evaluated the contribution of each analytical stage.

While PCG signal presents a challenging problem due to the fact that there is a significant spectral and temporal overlap of sounds originated from different cardiac structures, the possible benefits of digital auscultation that will be useful to the diagnosis of cardiac disorders and saving lives is gaining an increasing interest in developing accurate and intelligent auscultation applications. Combining the availability of electronic stethoscope with the advances in digital signal processing methods allows us to automate diagnosis of cardiac dysfunction as early as possible.

1.3 Scope and Objective

The main goal of this work is to design a method to analyze PCG with the aim of de-noising the signals using wavelet transformation and detect a single cardiac cycle in PCG signal. Features are extracted is accomplished by using Hilbert-Huang transformation and with the aid of support vector machine (SVM) classifier, we perform heart sounds classification. We verify our proposed system using MATLAB

and real murmur signals from the database of PCG signals at <http://www.peterjbentley.com/heartchallenge/#downloads> [8].

1.4 Thesis Organization

The first chapter introduces the motivations and objectives of thesis and summary on pertinent literature.

Chapter2 will describe the background knowledge about cardiovascular physiology and the characteristics of heart sounds and murmurs.

Chapter 3 presents a wavelet threshold de-noising method and Chapter 4 describe a method for heart sound segmentation based on the normalized average Shannon energy.

In Chapter 5 we will give an algorithm focusing on the feature extraction and classification of PCG. Experimental results are given in Chapter 6 while summary, conclusions are presented in chapter VII.

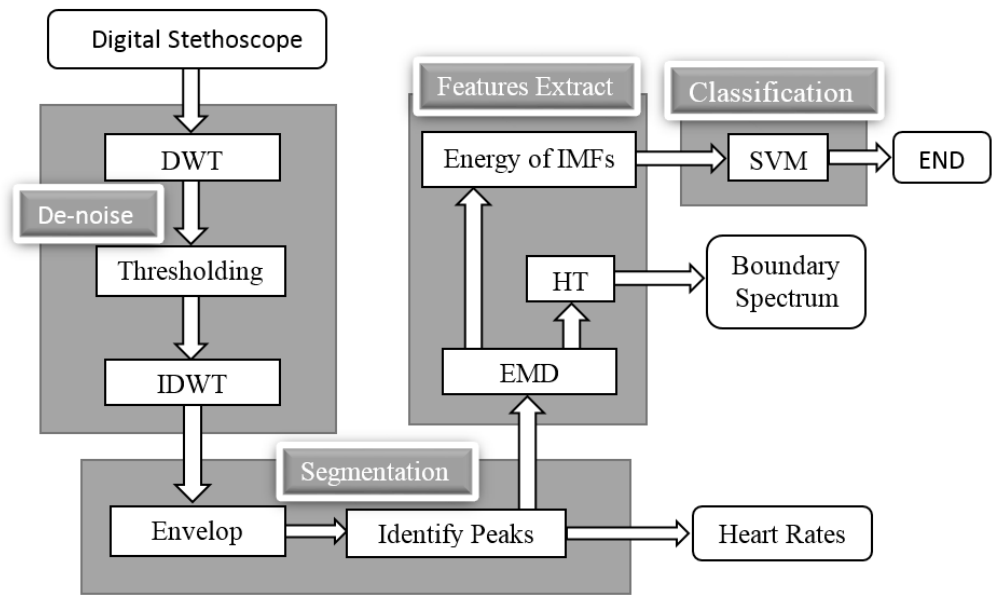


Figure 2. Flowchart of thesis work

CHAPTER II

HEART AND HEART SOUNDS

2.1 Cardiac Physiology

Heart is one of the most important organs in the cardiovascular system. The main function of the heart is to push adequate blood to the organs, tissues and cells. Blood will supply oxygen and nutrients, and take away the waste products (such as carbon dioxide, inorganic salt, etc.), which maintain the normal metabolism. The heart is located in the chest and sits a little to the left. It is about the size of a fist and weights between 200 to 425 grams[2].

Figure. 3 shows the anatomy of the human heart. The heart is divided into two parts by the septum: the left side and the right side. The heart consists four chambers: the right auricle, the right ventricle, the left auricle and the left ventricle. The valves between the auricle and the ventricles are called atrioventricular (AV) valves. The left one is mitral valve and the right one is tricuspid valve. There are heart valves between the ventricles and the major arteries. The pulmonary valve controls the blood from the right ventricle into the pulmonary artery and the aortic valve regulates blood from the left ventricle into the aorta.

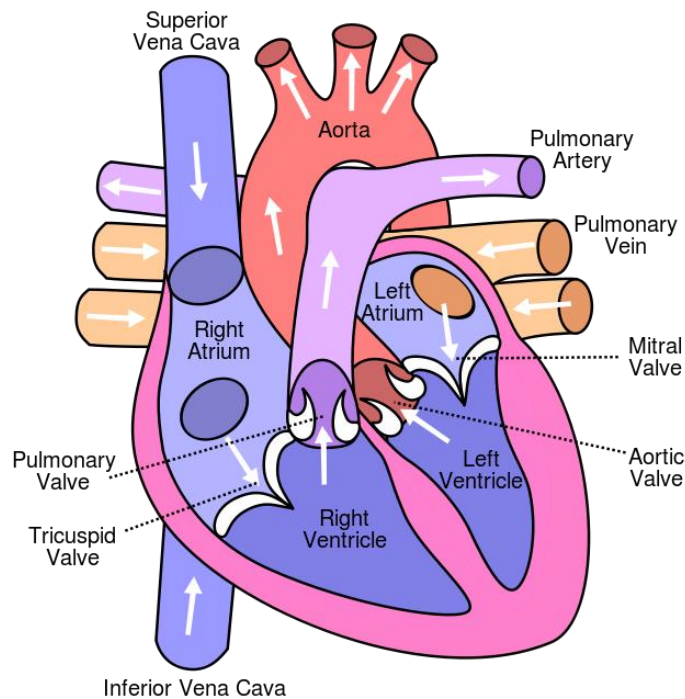


Figure 3. The anatomy of the human heart [9]

A cardiac cycle is defined as a complete heartbeat, it includes the diastole, the systole, and the intervening pause. First, the blood from the body and lungs enter the right and left auricles. While the atria are almost filled, the atria contract and the AV valves are partially open, pumping the blood into the ventricles. As the atria begin to diastole, the ventricles contract to pump blood into the arteries. The ventricles contract is called systole. The ventricles relaxation is called diastole.

2.2 Heart Sounds

Heart sounds are produced from the beat of muscles, the opening and the closure of the valves and the flow of blood. Medically, the cardiac cycle consists of

four major sounds: the first heart sound, the second heart sound, the third heart sound and the fourth heart sound. Figure.4 shows the four heart sounds in a cardiac cycle.

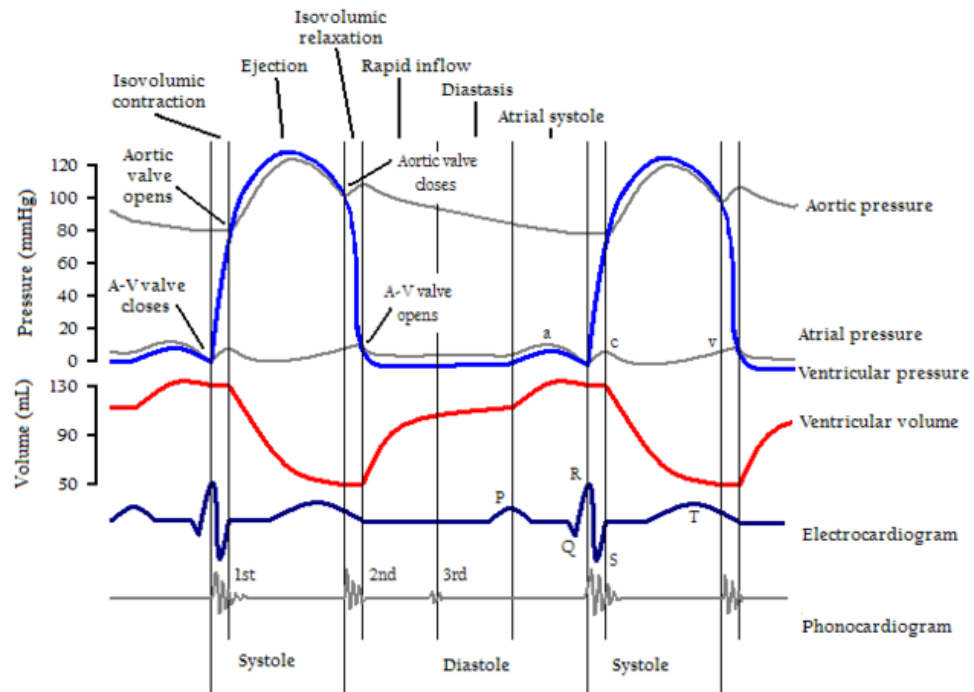


Figure 4. The sequence of cardiac cycle (PCG ECG and the pressure) [7]

The first heart sound results from three major parts: 1) the beginning of left ventricular contraction, 2) the abrupt tension on the AV valve as it finishes closing, 3) the acceleration of blood into the great vessels. S1 lasts from 100ms to 160ms. Its frequency components are in the range of 10-150Hz. S1 has the longer duration and higher amplitude than other heart sounds.

The second heart sound is caused by the closure of the aortic valve and pulmonary valve and the sudden reversing blood. S2 is split into two separate components, one due to the closure of the aortic valve (A2) and the other due to the

closure of the pulmonary valve (P2). S2 lasts from 60ms to 120ms. The frequency of S2 is usually higher than S1.

The third heart sound is a low frequency transient occurring during rapid ventricular filling during early diastole. The fourth heart sound is similar to the third heart sound that occurs at the time of atrial contraction, in the end of diastole. S3 and S4 are seldom audible in normal auscultation, but can be detected by phonocardiography systems with high sensitive sensors.

2.3 Heart Murmurs

When we talking about the cardiac murmurs, it is widely accepted that the turbulence of cardiac abnormalities causes all murmurs. There are three basic ways that turbulence occurs: 1) high rate of flow through normal or abnormal orifices, 2) blood flow into a dilated vessel or chamber, 3) backward flow through an incompetent valve or septal defect. Nevertheless, there are some murmurs are not pathological. Innocent heart murmurs are sounds made by the blood circulating through the heart's chambers and valves or blood vessels near the heart. There are two main cardiac murmurs, which are systolic murmurs and diastolic murmurs. The classification based on the position of murmur respect to the first heart sound and the second heart sound. Systolic murmurs occur between S1 and S2, while diastolic murmurs occur after S2.

Because of the huge abnormalities that can exist in cardiac structures, cardiac murmurs show a large amount of information. This thesis just lists some common types of murmurs and discusses their origin, shape and timing characteristics.

A: Innocent Systolic Ejection Murmur

PCG Shape: Figure 5 shows two possible shapes of innocent systolic ejection murmurs.

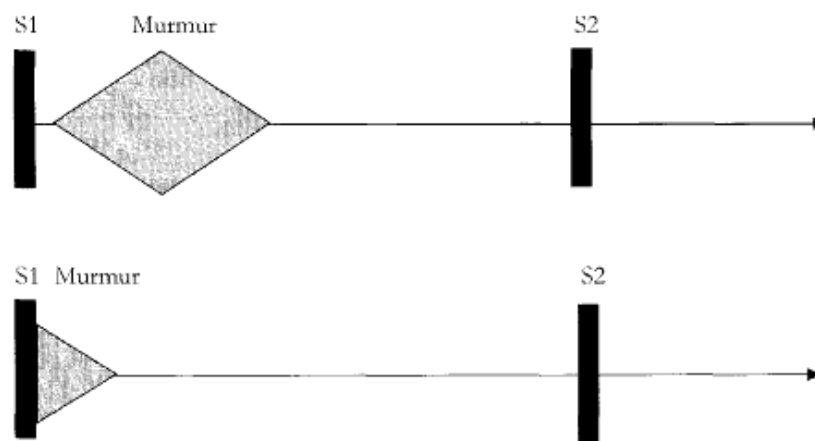


Figure 5. Shapes of an innocent systolic ejection murmur

Timing: Innocent systolic ejection murmur reaches its peak intensity in the first half of systole and ends well before S2 sound.

Pathology: Innocent systolic ejection murmurs are generally aortic in origin.

B: Mid-systolic Ejection Murmurs

PCG Shape: Figure 6 shows the possible shape of mid-systolic ejection murmurs.

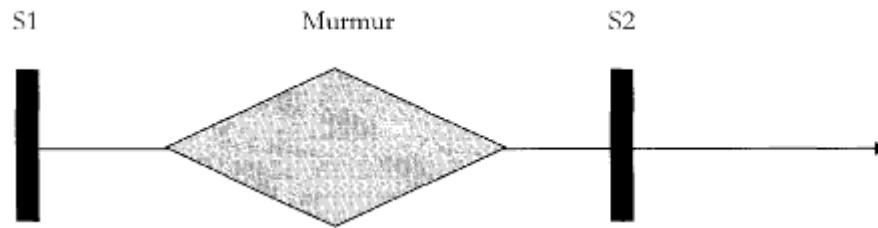


Figure 6. Shape of an ejection murmur

Timing: Mid-systolic ejection murmurs begin after S1 and reach peak intensity during mid-systole at the time of max blood ejection.

Pathology: Semilunar valve stenosis, increased rate of ventricular ejection or dilation of the aorta or pulmonary artery distal to the semilunar valve.

C: Insufficiency of Pulmonary Valve

PCG Shape: Figure 7 shows the possible shape of murmur of Insufficiency of Pulmonary Valve.

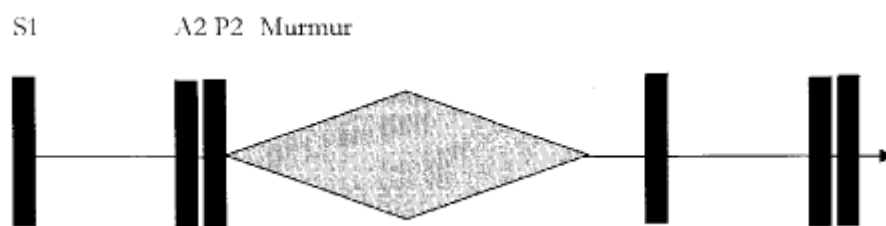


Figure 7. Pulmonary insufficiency in absence of pulmonary hypertension

Timing: The murmur of insufficiency of pulmonary valve often begins shortly after P2 and ends before S1.

Pathology: Backward flow of blood through pulmonary valve.

CHAPTER III

WAVELET BASED DENOSING OF HEART SOUND

3.1 Introduction to Wavelet Analysis

Heart sound signal is a typical biomedical signal, which is random and has a strong background noise. In the process to collect heart sound signals it is vulnerable to external acoustic signals and electrical noise interference, in particular, the friction caused by subjects breathing or body movement[10]. Wavelet transform is a time-frequency signal analysis method based on Fourier transforms [5]. It has good localization in both frequency and time domains. The word wavelet mean small wave, the wavelet transform decomposes the signal into one single function, called mother wavelet. The discrete wavelet transform (DWT) has been widely used in biomedical signal process. The DWT analyses a finite length time domain signal in different frequency bands, so we can decompose the signal into approximation and detail information.

3.2 Wavelet Threshold De-noising

Using wavelet methods in de-noising, is an important application of wavelet analysis. When we assume the random errors in signals are present over all the coefficients, we can use a threshold function in the wavelet domain to keep most coefficients representing signals, while the noise will tend to zero.

In mathematically, we measure a noisy signal

$$x = s + n \quad (3.1)$$

where n is an independent and identically distributed (iid) random noise (white noise).

So, the wavelet transform as:

$$y = W^T x = W^T s + W^T n = p + z \quad (3.2)$$

where p is the wavelet coefficients of signal s , consisting of the approximation and detail coefficients and z is wavelet coefficients of iid $N(0, 1)$.

$$\hat{s} = \Delta W y \quad (3.3)$$

Where \hat{s} estimate of s from y .

Assume a prior, we define the risk measure

$$R_{id}(\hat{s}, s) = E[\|s - \hat{s}\|_2^2] = \sum_{i=1}^n \min(s^2, \varepsilon^2) \quad (3.4)$$

Where ε is called the shrinkage factor.

Due to the effect of the shrinkage factor, we know that small coefficients of signals are set early to 0, and large coefficients are unaltered. So, the coefficients with small magnitude can be considered as pure noise and should be set to zero.

The steps are as follow: 1) getting wavelet coefficients from the original noise data after wavelet transformation, 2) Producing new wavelet coefficients from the threshold functions, 3) Applying the inverse wavelet transform to obtain clean signal

The key of wavelet de-noising is how to choose a threshold and how to use threshold to deal with wavelet coefficients. Usually wavelet threshold de-noising method includes:

A: Hard threshold function

Hard threshold function expression is as follows:

$$y(x) = \begin{cases} x, & |x| \geq T \\ 0, & |x| < T \end{cases} \quad (3.5)$$

B: Soft-threshold function

Soft-threshold function expresses as follows:

$$y(x) = \begin{cases} \text{sgn}(x)(|x| - T), & |x| \geq T \\ 0, & |x| < T \end{cases} \quad (3.6)$$

C: Two variables threshold function

Two variables threshold function expresses as follows:

$$y(x) = \begin{cases} x - T + \text{karctan}(bT^{2a+1}), & x \geq T \\ \text{karctan}(bT^{2a+1}), & |x| < T \\ x + T - \text{karctan}(bT^{2a+1}), & x \leq -T \end{cases} \quad (3.7)$$

Where,

$$b = \frac{2a+1+m\sqrt{(2a+1)^2-\pi^2}}{\pi T^{2a+1}} \quad (3.8)$$

$$k = \frac{1+(bT^{2a+1})^2}{(2a+1)bT^{2a}} \quad (3.9)$$

Where, $a > 0$ and a is an integer; $-1 \leq m \leq 1$.

Hard threshold function only processes the wavelet coefficients smaller than the threshold and left alone others. What is more, hard threshold function has two break points at T and $-T$. Soft-threshold function doesn't have the break point problem. However, soft threshold function reduces the absolute value of the wavelet coefficients, resulting in a certain loss of high frequency information.

In two variables threshold function, when $m = -1$, the threshold function can be regarded as the similar soft-threshold function and while $a \rightarrow \infty$ it is the soft-threshold function; when $m = 1$, the threshold function likes the hard-threshold function, and while $a \rightarrow \infty$ it is the hard-threshold function. So, we can use variables 'm' and 'a' to adjust the deviation.

3.3 Wavelet Based De-noising Experiment

In order to illustrate performance of wavelet based de-noising methods, we use complex exponential signals as the test signals, the formula is:

$$f(t) = Ae^{-t/\tau} \sin(2\pi f_c t) \quad (3.10)$$

Where A is amplitude, τ is attenuation constant, f_c is oscillation frequency.

Figure. 8 shows the waveform of complex exponential signals. We add the low-intensity Gauss noises to the test signals ($\text{SNR} = 25$). Then, we use three wavelet

threshold methods to reduce the noise. In the experiment, we use db6 wavelet to decompose the signals, and the two variables are $a=0.5$, $m=0.5$ [11].

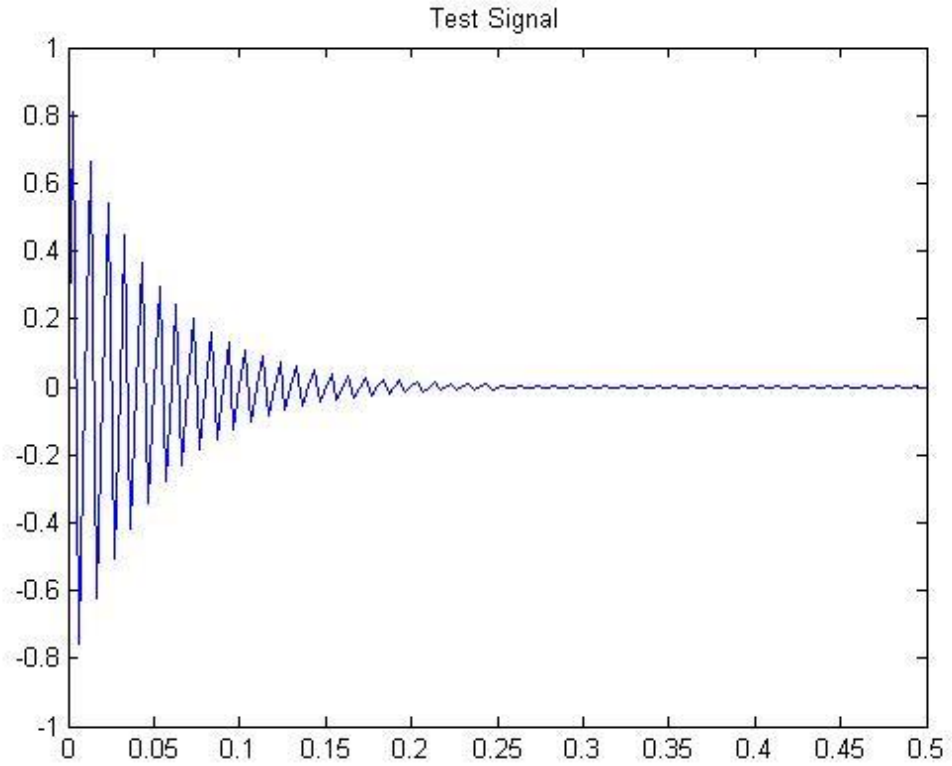


Figure 8. The waveform of the test complex exponential signals

In Figure. 9, we can see that result of soft-threshold method is smoother than that of hard-threshold method. While the last two methods both lost some useful information, the simulation result indicates that the two variables threshold function can get better de-nosing result.

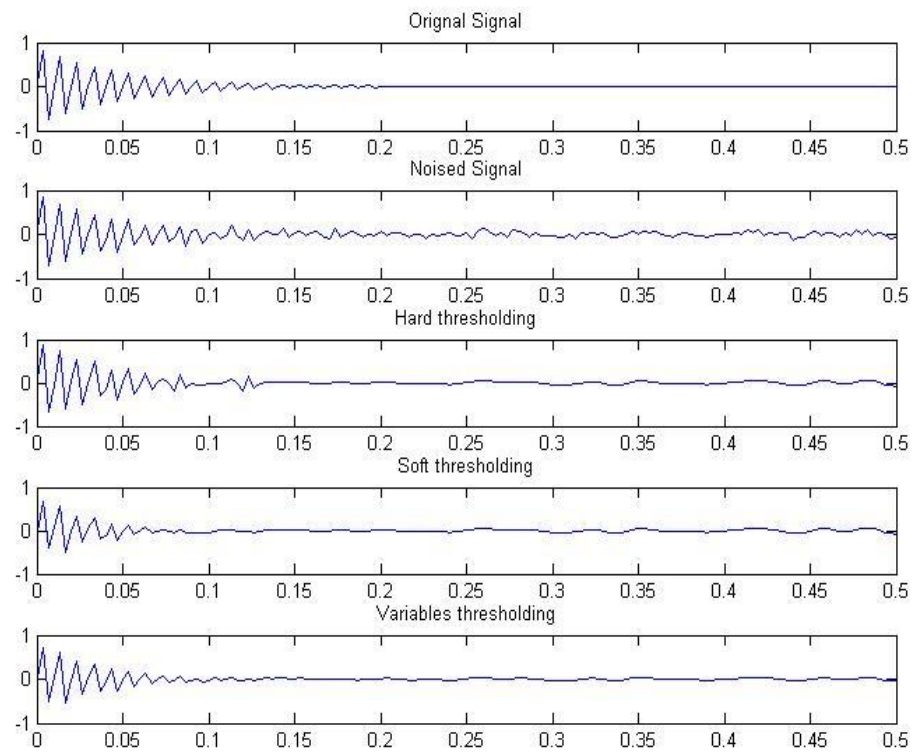


Figure 9. Result of the wavelet threshold de-noising experiment

CHAPTER IV

SEGMENTATION OF HEART SOUND

Usually, a cardiac cycle splits into the first heart sound, the systolic period, the second heart sound and diastolic period. Before we analysis the heart sound, we should segment the phonocardiogram signal at first. If we analysis the whole phonocardiogram signal, it is not only a waste of time, but also meaningless. Now there are many heart sound signals segmentation algorithm, some of them are using electrocardiogram (ECG) as reference to identify the components of heart sound, it is not convenient because of the additional hardware requirement. Some segmentation is based on the frequency-domain characteristics of the heart sound signals, such as Zaeemzadeh[12]. In this chapter, we will give an algorithm based on the normalized average Shannon energy [5]. This algorithm does not need any reference signal, and considering the diversity and complexity of heart sound.

4.1 Method

Before we segment the heart sounds, we should get the envelope of sounds signals. In order to make the low intensity sounds easier to be found, we use the normalized average Shannon energy. It calculates as follow

A: the de-noising signal $x(k)$ is normalized to $x(k)_{norm}$ as

$$x_{norm}(k) = (x(k))/(\max(x(k))) \quad (4.1)$$

B: the signal $x_{\text{norm}}(k)$ are segmented in continues $2t$ time. As shown in Figure.

10, two adjacent sections are overlap in one t ($t=0.01\text{s}$). The average Shannon energy of each section is calculated as

$$E_{\text{norm}}(t) = -1/N \times \sum_{k=1}^N x_{\text{norm}}^2(k) \cdot \log [x_{\text{norm}}^2(k)] \quad (4.2)$$

Where N is the number of signal points in a section.

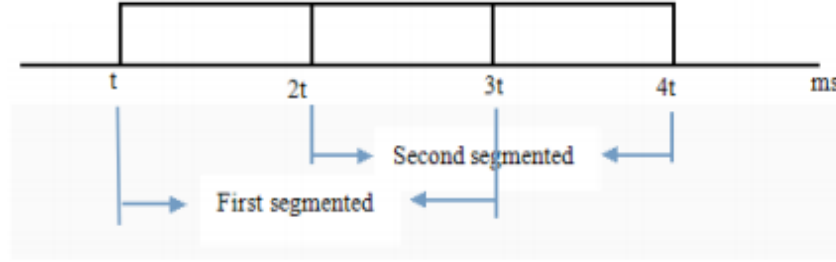


Figure 10. The overlap between two adjacent sections

C: The normalized average Shannon energy is computed according to,

$$P(t) = (E_{\text{norm}}(t) - M(E_{\text{norm}}(t))) / (S(E_{\text{norm}}(t))) \quad (4.3)$$

Where, $M(E_{\text{norm}}(t))$ is the mean value of $E_{\text{norm}}(t)$; $S(E_{\text{norm}}(t))$ is the standard deviation of $E_{\text{norm}}(t)$.

Based on the envelope curves, we pick up the peaks of $S1$ and $S2$ at first, then we locate the first heart sound, the systolic period, the second heart sound and diastolic period. The step as followed:

Step.1: Picking up peaks of S1 and S2

We pick up the peaks of S1 and S2 by a selected threshold in the envelop curve.

Due to the amplitude of some heart sounds are very low, the initial fixed threshold is set to the quarter of maximum value of envelope curve.

Step.2: Rejecting extra peaks

There are some extra peaks may be caused by murmurs and splitting heart sounds of S2. In order to eliminate the extra peaks, the intervals between each adjacent peaks are calculated[5]. If the interval of two adjacent is less than the minor of average of 10 interval and 0.25s, we will judge one of these two adjacent peaks is an extra peaks. We will try to pick up the larger peak and test by the new intervals. If the test passed, we pick up the larger one, otherwise, the smaller one is picked up.

Step.3: Recovering weak peaks of S1 or S2

Some second heart sounds are so weak that their energies are less than the threshold. To find the lost peaks, we still examine the intervals between the adjacent peaks. When the intervals of two adjacent peaks exceed 0.9s, it is assumed that a peak has been lost. We will pick up the maximum point of intervals as heart sound.

Step.4: Identifying the peaks of S1 or S2

The identification is based on the two facts: 1) the diastolic period is longer than systolic period; 2) the systolic period is relatively constant. According to these, we

examine the intervals both forwards and backwards to maintain the relative consistency of systolic and diastolic intervals. When we confirm the systolic and diastolic intervals, the heart sounds before the systolic period are the first heart sounds. The heart sounds after the systolic period are the second heart sounds.

Step.5: Determine duration of S1 and S2

The detected peaks indicate the approximate location of heart sounds. The duration of these sounds are calculated by other defined boundaries thresholds. From the chapter 2, the duration of S1 is about from 100 to 160ms, while the S2 is about from 60 to 120ms. We modified the thresholds by confining the duration of heart sounds between the medical ranges.

4.2 Results and Discussion

Phonocardiography from the datasets of [8] (sponsored by PASCAL) were used to verify the accuracy of the proposed method. We select 35 records of normal heart sound and 45 records abnormal heart sound (means the patients with heart failure or heart disease) to segment. The example results are shown in Figure 11-13. The signal in Figure 11 is normal heart sound, while Figure12 and Figure 13 present the segmentation of abnormal heart sound.

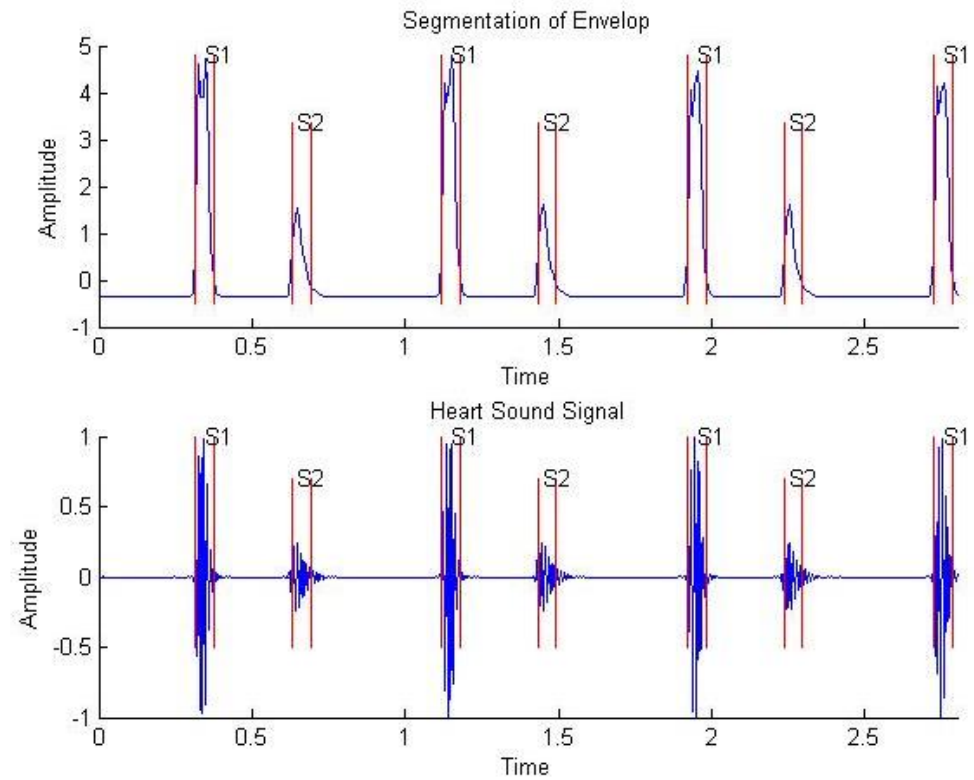


Figure 11. Detection of Single S1 S2 in normal heart sound

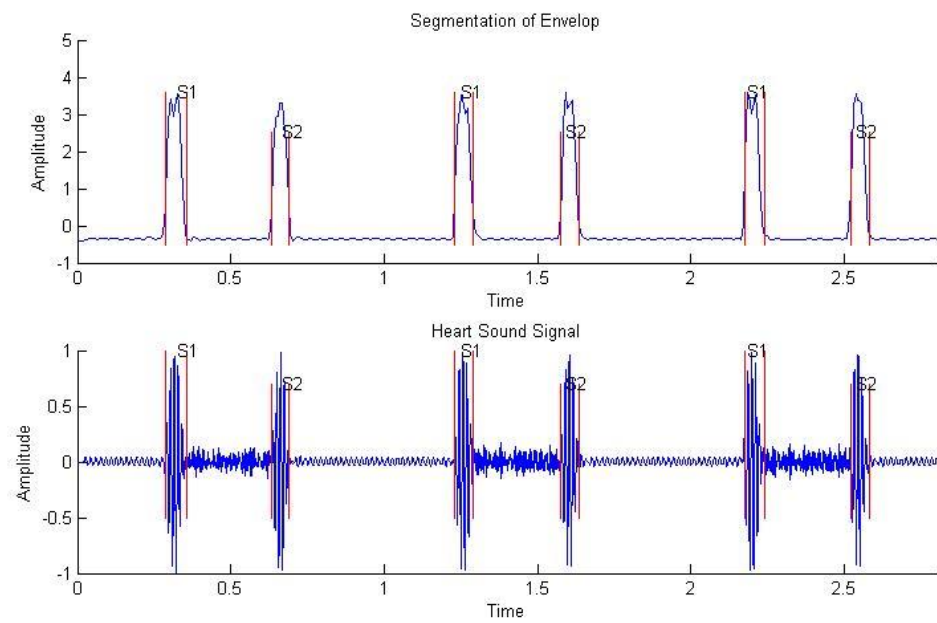


Figure 12. Detection of heart sound with Holo Systolic Murmur

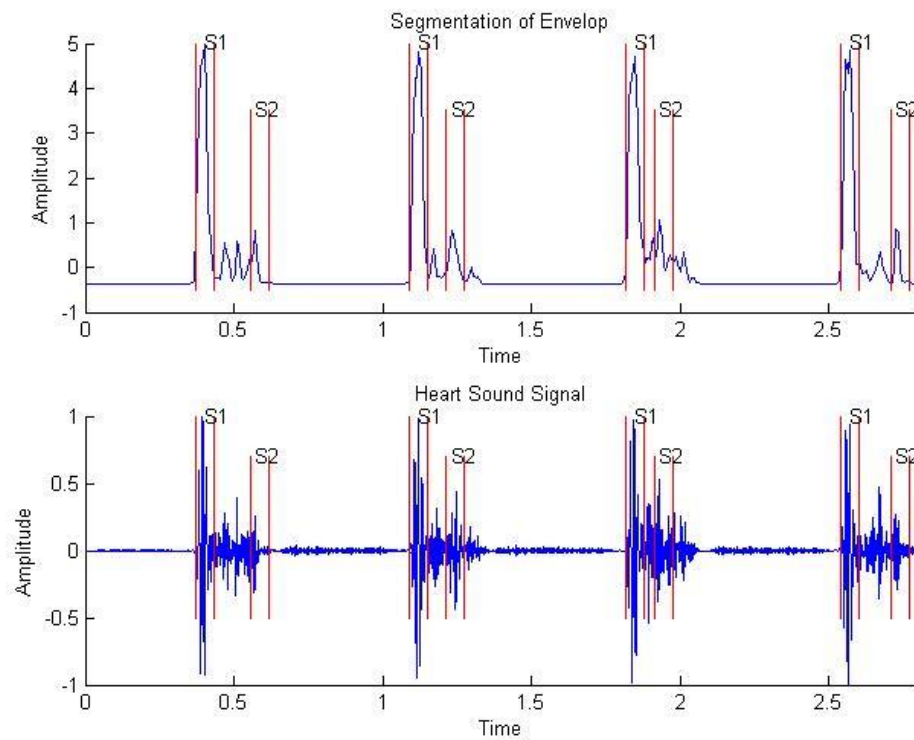


Figure 13. Detection of heart sound with Systolic and Diastolic Murmurs

The results are summarized in Table.1

Table 1. The result of heart sounds segmentation

	Normal Heart Sounds	Abnormal Heart Sounds
Number of cases	10	11
Correct number	10	9
Correct Ratio (%)	100	81.81

Table 1 shows most normal heart sounds are segmented correctly. Seven recordings of 55 abnormal heart sounds are wrongly processed. The results of the experiment indicate 88.75 % correctness in all heart sounds segmentation.

Experimental results show that the proposed method is validated to perform well for both normal and typical abnormal heart sounds.

CHAPTER V

FEATURE EXTRACTION AND CLASSIFICATION

5.1 Introduction

In order to classify heart sounds into pathological or innocent sounds, this paper uses Hilbert-Huang Transformation (HHT) method to analyze the Phonocardiogram Signals [13]. The HHT gives an exact frequency-energy distribution, we extract the energy ratio of high-low frequency as the feature vector. Classification of the signal features is achieved using Support Vector Machine (SVM), which is an effective technique in high dimensional spaces [14]. The classifier is trained with small dataset and testes on high-dimensional feature space.

5.2 Hilbert-Huang Transformation

The Hilbert-Huang transform (HHT) was developed by Huang for the transient and non-stationary signal. The method provides highly efficient, adaptive algorithm for signal processing. HHT method contains two steps: empirical mode decomposition (EMD) and Hilbert Spectral Analysis (HSA). The central part of the HHT is EMD which allows the signal to be decomposed into finite Intrinsic Mode Functions (IMF) and a final residue after sifting process.

The intrinsic mode function is defined by the following two conditions:

1. In the whole dataset, the number of extrema and the number of zero-crossings must be equal or differ at most by one.
2. At any time, the mean value of envelop defined by the local maxima and envelop of the local minima must be zero.

These conditions guarantee a well-behaved Hilbert transform of the IMF. The sums of all IMFs match the original signal. Performing the Hilbert transform to each of the IMFs allows us to determine the instantaneous frequency and instantaneous amplitude of the signal.

By using EMD method, the input signal $X(t)$ can be decomposed as

$$X(t) = \sum_{i=1}^n C_i(t) + r_n(t) \quad (5.1)$$

where $C_i(t)$ is the i th IMF, $r(t)$ is the final residue function, and n is the number of IMFs. In Figure 14, we show the process of IMFs computing. Comparing HHT with other methods on signal decomposition such as Fourier and wavelet transforms, one find a very unique quality in HHT, HHT base functions come from the signal directly. Indeed, HHT is a very adaptive transform and guarantees to preserve the inherent characteristic of the signal and avoids the diffusion and leakage of the signal energy as happens in other methods [13].

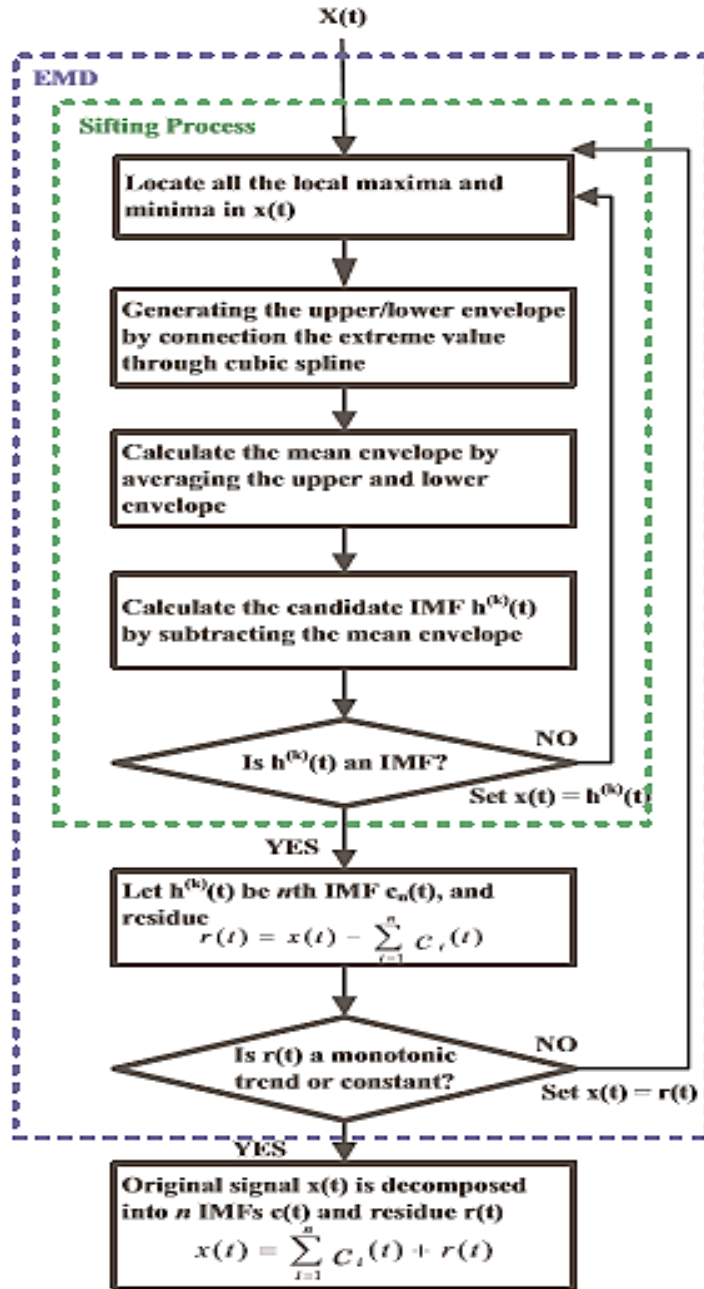


Figure 14. The Process of computing HHT IMFs [12]

Once EMD process is completed, IMFs are transformed into time-frequency spectrum through Hilbert transformation.

$$Y(t) = \frac{1}{\pi} P \int \frac{X(t')}{t-t'} dt' \quad (5.2)$$

where P denotes the Cauchy Principal Value, X(t) is the given input function, and Y(t) is the Hilbert transformation of the input signal.

With equation 5.2, X(t) and Y(t) can be combined to form the analytical signal Z(t) given by

$$Z(t) = X(t) + jY(t) = a(t)e^{j\theta(t)} \quad (5.3)$$

where a(t) is the function of time-dependent amplitude and $\theta(t)$ is the function of time-dependent phase. Also, the instantaneous frequency can be defined as

$$\omega(t) = d\theta(t)/dt \quad (5.4)$$

Therefore, one can express the original signal by the following equation:

$$X(t) = Re\{ \sum_{i=1}^n a_i e^{i \int \omega_i(t) dt} \} \quad (5.5)$$

where *Re* equals real part of the value to be calculated. The frequency-time distribution of the amplitude is designated as the Hilbert Amplitude Spectrum, H (ω, t), or simply Hilbert boundary spectrum, defined as

$$H(\omega, t) = \sum_{i=1}^n a_i(t) \quad (5.6)$$

With the Hilbert spectrum defined in equation 5.6, we can also define the marginal spectrum h (ω), as

$$h(\omega) = \int_0^T H(\omega, t) dt \quad (5.7)$$

where T is the time duration of data segment.

5.3 Support Vector Machine

Support Vector Machines (SVM) have been successfully applied to classification, regression and pattern recognition since introduced by Vapnik [14]. The mechanism is constructing the optimal classification hyperplane to make the interval between classifications maximum, which is based on the training data and the decision boundary. SVM reduces the compromise of dimensional disaster, therefore can be used to deal with the nonlinear and high dimensional data[15].

1) A: Linear and Non-linear Classifier of SVM

When sample is linear separable, we construct a hyperplane or a set of hyperplanes that separate the data. In Figure. 15, we consider the samples from the class 1 that satisfy the equation:

$$w^T x + b = 1 \quad (5.8)$$

Similarly, the samples from the class -1 satisfy the equality

$$w^T x - b = -1 \quad (5.9)$$

where x is the trained data point, w is the vector and b is a bias term, w and b define a boundary that separate the points. Depending upon the sign of the function, an input x is classified into either of the two classes. If the function is positive, the input is

classified as its own class, otherwise it is classified as the other class. The distance between hyperplane is $2/|w|$, we can see that the identification of the optimum separation hyperplane is performed by maximizing $2/|w|$.

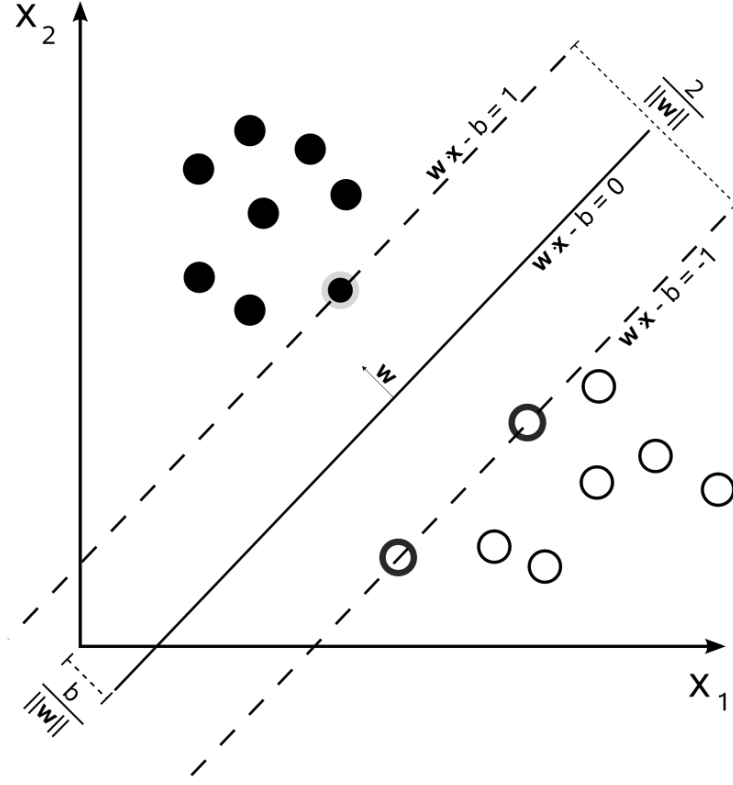


Figure 15. Maximum-Margin hyperplane and margins for an SVM trained with samples from two classes [16]

The problem becomes a quadratic programming optimization problem with the task to

$$\min | \frac{1}{2} w^T \cdot w | \quad (5.10)$$

Subject to

$$y_i(w^T \cdot x_i + b) \geq 1 \quad (5.11)$$

where x is the trained data point, w is the vector and b is a bias term, i is the number of trained data point

Hence, minimizing the previous constrained problem is equivalent to

$$\max \bar{Q}(\lambda) = -\frac{1}{2} \sum_{i,j=1}^N \lambda_i \lambda_j y_i y_j x_i^T x_j + \sum_{i=1}^N \lambda_i \quad (5.12)$$

Subject to

$$\sum_{i=1}^N \lambda_i y_i = 0 \quad (5.13)$$

where x is the trained data point, y is the indicating class of the x , λ is Lagrange Multiplier, and $i = 1, 2, 3, \dots$

This problem can now be solved by standard quadratic programming with Lagrange multipliers. If λ is the optimal Lagrange multiplier, we get the decision function:

$$f(x) = \text{sgn}\{ \sum_{i=1}^N \lambda_i y_i (x_i \cdot x) + b \} \quad (5.14)$$

where $b = \sum_{i=1}^N \lambda_i y_i x_i \cdot x_i$ as defined also with equation 5.xx

When the training set are non-linear separable, that every dot product is replaced by the inner product computation which is referred to as the kernel function. This allows the SVM to fit the maximum-margin hyper plane in a transformed feature space.

2) Basic kernel functions

SVM algorithm uses Kernel function to map the training data into kernel space. Many kernel functions have been proposed in the literature [16] such as the traditional ones:

$$\text{Linear kernel: } k(x, y) = x^T \cdot y \quad (5.15)$$

$$\text{Sigmoid kernel: } k(x, y) = \tanh(x^T \cdot y - \theta) \quad (5.16)$$

$$\text{Gaussian Radial Basis Function kernel: } k(x, y) = \exp * \left(-\frac{\|x-y\|^2}{2\sigma^2}\right) \quad (5.17)$$

And many others such as Quadratic kernel, Multilayer Perceptron kernel, and K-type kernel. All kernel function introduce at least one kernel parameter to control the complexity of the kernel function.

CHAPTER VI

SIMULATIONS AND EXPERIMENT RESULTS

6.1 Heart Sound Analysis by HHT

In Figure. 16 and Figure 17, we show the IMFs of normal heart sound and abnormal heart sound, respectively, which is a needed step in order to obtain the signals Hilbert's spectrum; as a result from decomposition using EMD method, that is by seeking its IMF. we know that the first heart sound mainly appears in the fourth and fifth IMF; the second heart sound mainly occur in the first, second, third and fourth IMF while the cardiac murmur mainly exist in the first and second IMF.

Hilbert spectrum of heart sound fully reveals the instantaneous frequency and amplitude when they vary with time dynamically. Thus, it shows that heart sound is mainly composed of low frequency components as results show in Figures 16 and Figure 17.

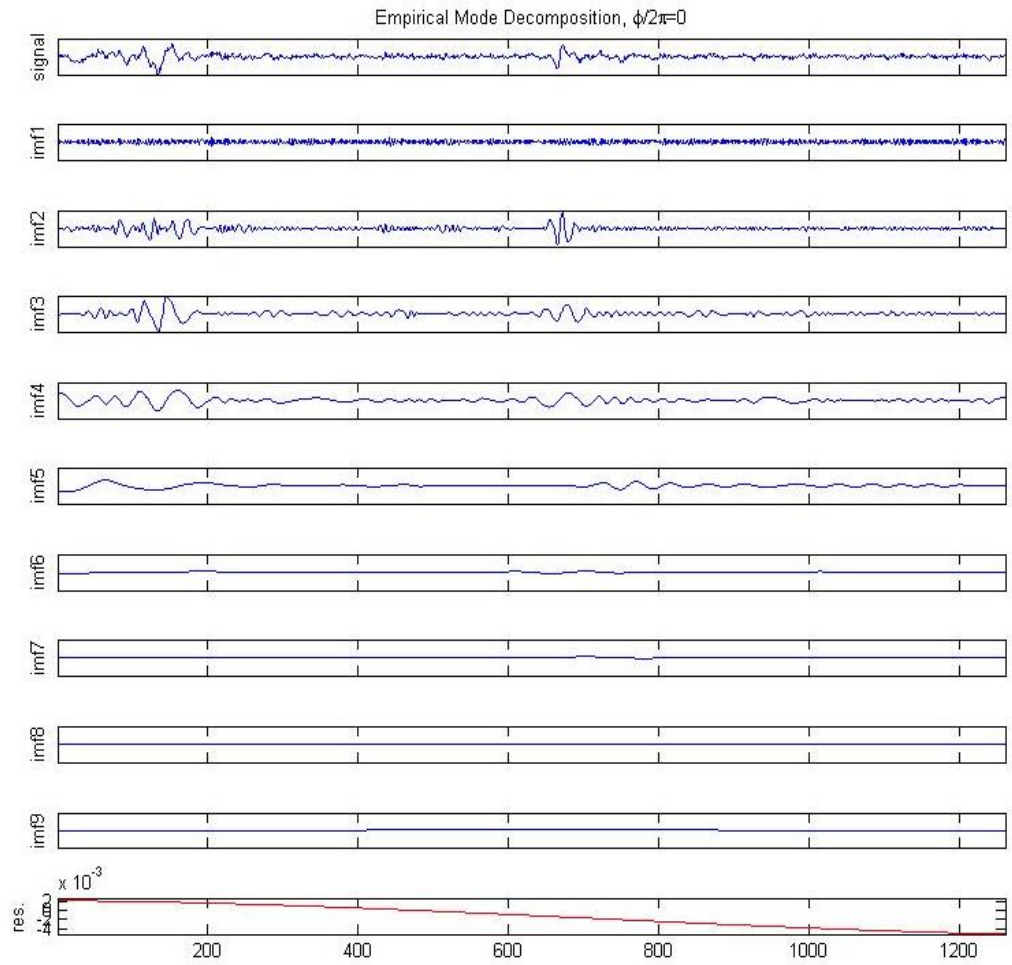


Figure 16. The empirical mode decomposition of normal heart sound. (row1) Data, (row2-10) nine IMF components, (row11) the final residue components

From Figure. 18, Hilbert boundary spectrum shows the energy distribution of normal heart sound changing with frequency. It has two main frequency peaks. The first peak locates around 40Hz, which is in the frequency range of S1. The second peak lies around 70Hz corresponding to the frequency range of S2.

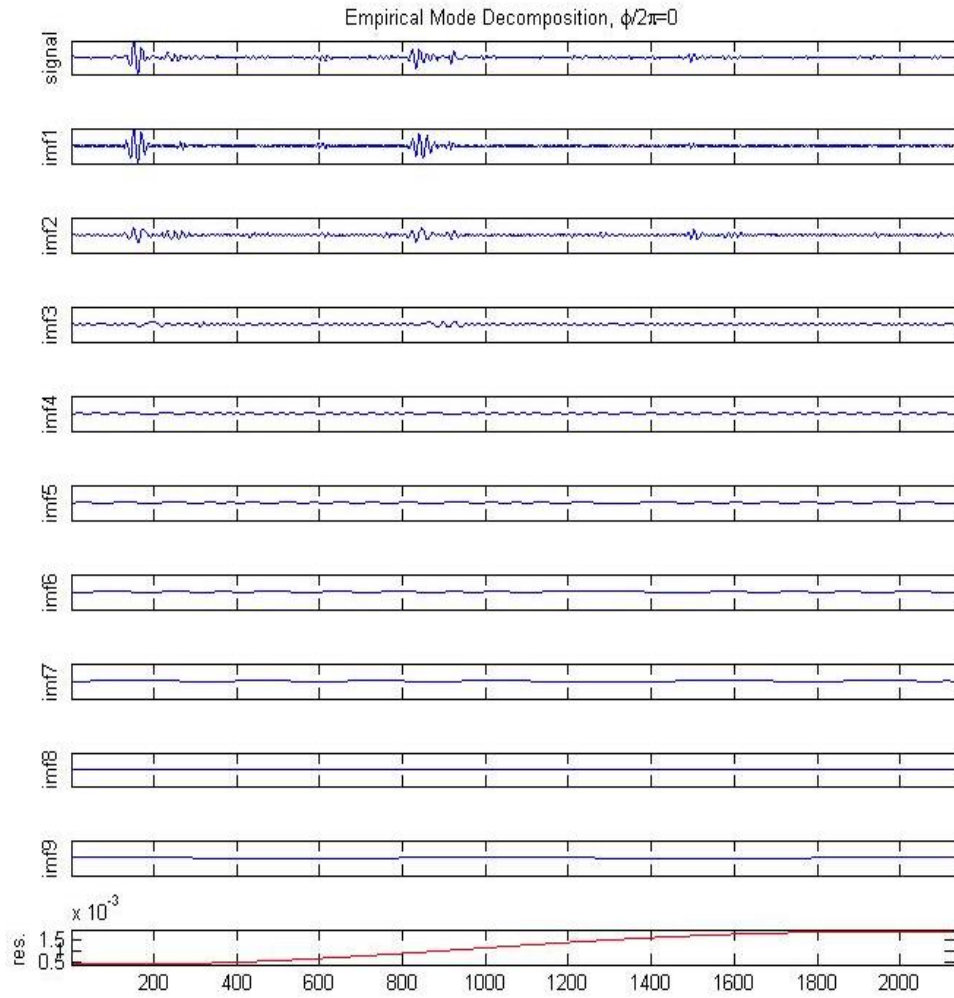


Figure 17. The empirical mode decomposition of abnormal heart sound. (row1) Data, (row2-10) nine IMF components, (row11) the final residue components

In Figure 19, we show the energy distribution of abnormal heart sound. There are three main frequency peaks. The first and second peaks are located around 40Hz and 70Hz corresponding to the frequency range of S1 and S2, respectively. The third peak lies around 120Hz, which is the frequency range of diastolic murmurs. It is worth noting that in normal conditions such higher frequency doesn't appeared in the normal heart sound.

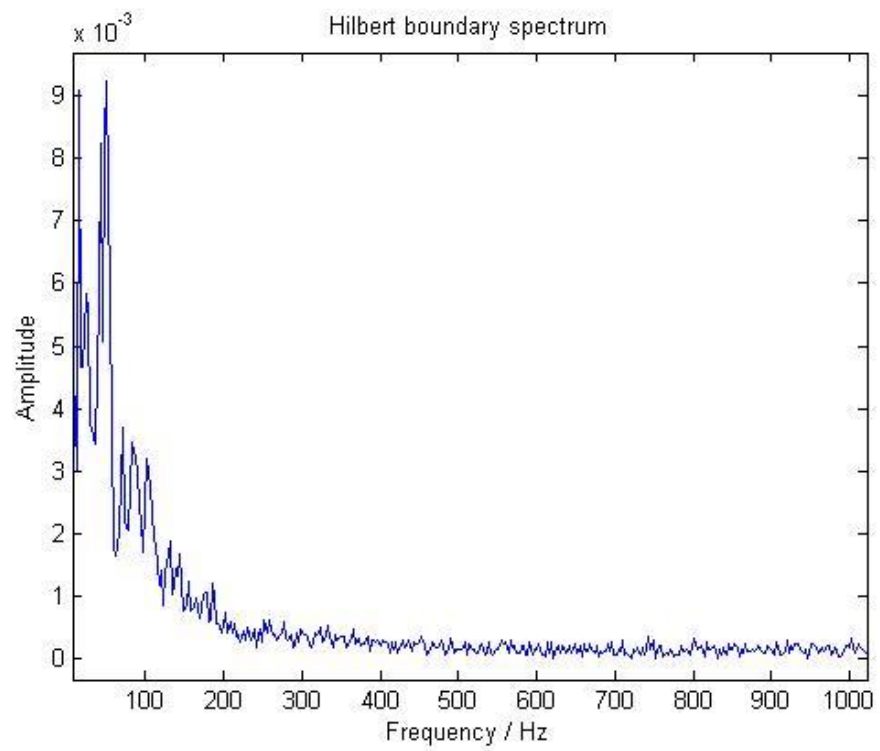


Figure 18. Hilbert boundary spectrum of the normal heart sound

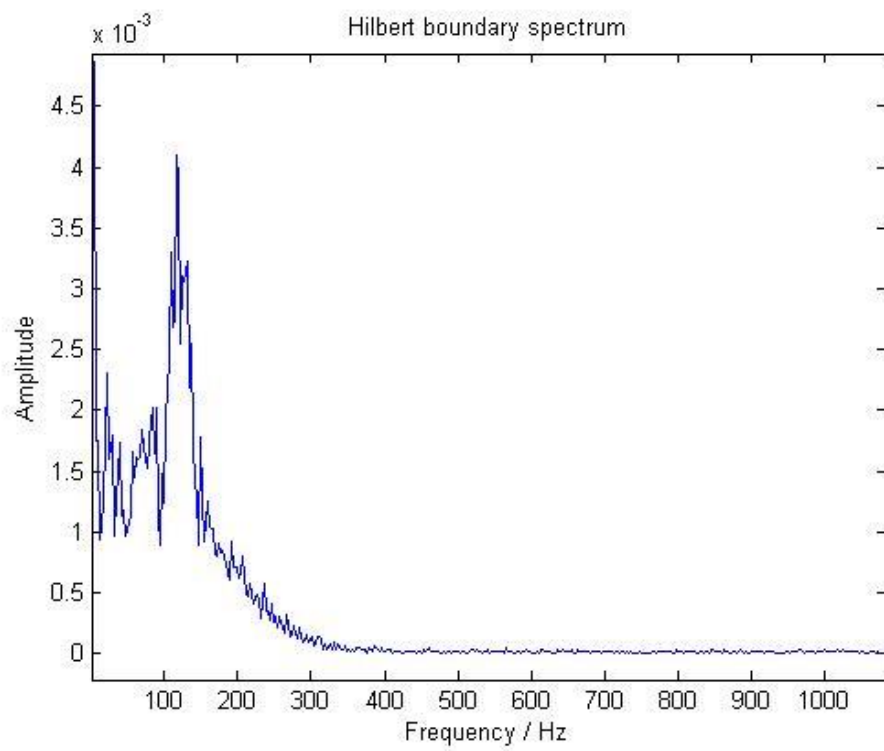


Figure 19. Hilbert boundary spectrum of the abnormal heart sound

6.2 Feature Extraction

The spectrum analysis of heart sound, we direct our algorithm to obtain the particular features of the heart sounds. Feature extraction is one of the most important steps because the performance of classifiers will degrade significantly if the features are not chosen properly. Due to the change of the energy of each IMF components, we can present the property of heart sounds. The instantaneous signal energy with different scales are used as to create our feature vector to be used in our effort to classify the normal and abnormal heart sounds.

The Feature extraction steps are as follows:

1: From the Figure 16 and Figure 17, we can find the values of IMF8 and IMF9 are tiny, so we select 7 former IMF components and then add the final residual component.

2: Calculate the total energy (E) of each component in a heart cycle using equation: $E_n = \sum |f_n|^2$

3: Construct the feature vector (T) with the 8 total energy value:

$$T = [E_1, E_2, E_3, E_4, E_5, E_6, E_7, E_R]$$

6.3 Heart Sound Classification

In Chapter 4, we obtained 71 samples of segmented PCG signals, 50 recordings are selected (including 23 normal cases and 27 abnormal cases) as the training set and the remaining 21 (including 10 normal cases and 11 abnormal cases) as the testing set. In this thesis, MATLAB libsvm toolbox (developed by Dr. Lin [16]) was used to implement the classification of heart sounds. We also used RBF kernel and two parameters σ and C needed. The parameter σ defines the width of the Gaussian kernel that influences the flexibility of the SVM classifier while C controls the width of the margin on each side of the separating hyperplane which influences the misclassification of the SVM classifier [17]. In order to optimize chosen values of σ and C parameters, we select the values for $\sigma = 0.3$ and $C = 5.0$.

Result of the classification of the test sets consisting of 21 cases are presented in Table 2. These results indicate that only 2 abnormal heart sound signals, out of the 11 abnormal signals, are recognized as normal heart sound signals with all other signals are accurately classified

Table 3 shows that accuracy of the SVM classification. From the results, it can be seen that SVM has a high accuracy even though we have a limited training sets. SVM has a strong adaptability to the small samples. Simulation results indicated that the proposed algorithm achieves the sought goal with a classification accuracy of 90.48% composed of 100% sensitivity and 81.8% specificity. However, we conclude

that due to the noticeable difference between normal and abnormal heart sounds in the selected features, the recognition rate of normal heart sounds reached 100 percent.

Therefore, the whole system need more heart sound signals to improve its performance.

Table 2. The result of the classification of the test sets consisting of 21 cases

No	E1	E2	E3	E4	E5	E6	E7	E8	Result	Fact
1	0.74	13.78	2.48	6.88	0.86	0.20	0.02	0.00	1	1
2	1.05	11.18	11.83	6.58	2.06	0.74	0.20	0.04	1	1
3	0.34	10.81	3.49	2.48	0.78	0.07	0.07	0.02	1	1
4	0.71	5.62	15.63	16.16	13.57	3.17	0.71	0.03	1	1
5	2.22	8.70	7.14	5.62	2.20	1.15	0.23	0.04	1	1
6	0.17	8.20	18.68	13.73	1.64	1.23	0.21	0.02	0	0
7	10.71	11.01	4.05	3.28	0.49	0.34	0.16	0.03	0	0
8	23.78	2.66	0.57	0.37	0.01	0.00	0.01	0.01	1	0
9	1.69	21.67	2.54	0.28	0.07	0.04	0.06	0.17	0	0
10	21.27	15.82	8.24	1.33	0.11	0.03	0.00	0.03	0	0
11	22.86	24.90	2.34	0.43	0.34	0.17	0.12	0.01	1	0
12	18.10	28.11	2.19	1.24	0.35	0.05	0.10	0.05	0	0
13	7.01	13.88	35.40	2.33	1.01	0.68	0.13	0.12	0	0
14	8.93	19.14	14.10	4.29	1.88	0.68	0.05	0.19	0	0
15	15.90	37.94	55.25	14.11	5.21	0.97	0.94	0.04	0	0
16	17.95	9.75	4.42	1.53	0.08	0.03	0.01	0.02	0	0
17	2.21	7.24	15.15	5.16	2.10	0.92	0.60	0.05	1	1
18	0.41	1.54	1.55	3.76	2.68	0.61	0.15	0.01	1	1
19	0.18	3.06	2.17	0.77	0.11	0.07	0.13	0.11	1	1
20	0.15	0.18	0.49	0.22	0.24	0.04	0.01	0.02	1	1
21	2.82	6.52	9.74	3.55	1.21	0.20	0.02	0.00	1	1

Table 3. The percentage accuracy of the SVM classification

	Ture Condition		
	Normal HS	Abnormal HS	Total
Predicted normal HS	10	2	12
Predicted abnormal HS	0	9	9
Totals	10	11	21
Accuracy:90.5% Sensitivity:100% Specificity:81.8%			

CHAPTER VII

CONCLUSIONS AND FUTURE WORK

This thesis focused on the problem phonocardiogram analysis as an aid tool to detect and diagnose any abnormalities of heart condition. With the above mentioned goal, we investigated a wide variety of fields ranging from cardiac auscultation, wavelet threshold de-noising, heart sound segmentation, Hilbert-Huang transform, feature extraction and classification by support vector machine.

We developed a wavelet based de-noising scheme that achieves a cleaner signal. We developed an energy-based segmentation method which is validated to perform well for both normal and typical abnormal heart sounds. We applied Hilbert-Huang Transform to analyze the heart sounds and calculate the energy of selected IMF components that enabled us to construct the feature vector. Finally, the classification goals was accomplished using Support Vector Machine. Simulation results indicated that the proposed algorithm achieves the sought goal with a classification accuracy of 90.48% composed of 100% sensitivity and 81.8% specificity.

Overall, a framework to classify normal and abnormal heart sounds is proposed using PCG. This system can be implemented in real time using PCG obtained from the new digital stethoscope technology and by the present state of the art embedded technology.

Other future suggestions can be to aim to further analyze the abnormal into the different classes of heart diseases. Indeed, this goal opens up several avenues for the further research to be more accurate. First, we need to have a deep explore in Cardiac physiology, which is the foundation of all research of heart auscultation to allow for better feature recognition. Second, with the current framework, one can add more features that could present a potential to classify the different murmur signals. We need to extract the features from time domain and frequency domain and combine it with other statistical characteristics to produce a thorough analysis of the framework performance versus the different features. Third, we suggest a multi-classifier such as Multiclass SVM can be very valuable in solving such a classification problem, with the key point is the ability to create a suitable decision tree of SVM.

BIBLIOGRAPHY

- [1] World Health Organization, *Global status report on noncommunicable diseases 2014*. 2014.
- [2] A. Leatham, "Auscultation and phonocardiography: a personal view of the past 40 years.," *Br. Heart J.*, vol. 57, pp. 397–403, 1987.
- [3] M. Tavel, "Classification of systolic murmurs: Still in search of a consensus," *Am. Heart J.*, vol. 134, no. 2, pp. 330–336, 1997.
- [4] L.-G. Durand, Y.-E. Langlois, T. Lanthier, R. Chiarella, P. Coppens, S. Carioto, and S. Bertrand-Bradley, "Spectral analysis and acoustic transmission of mitral and aortic valve closure sounds in dogs," *Med. Biol. Eng. Comput.*, vol. 28, no. 5, pp. 439–445, Sep. 1990.
- [5] H. Liang and I. Hartimo, "A heart sound feature extraction algorithm based on waveletdecomposition and reconstruction," *Proc. 20th Annu. Int. Conf. IEEE Eng. Med. Biol. Soc. Vol.20 Biomed. Eng. Towar. Year 2000 Beyond (Cat. No.98CH36286)*, vol. 3, no. 3, pp. 1539–1542, 1998.
- [6] B. Popov, G. Sierra, L. G. Durand, J. Xu, P. Pibarot, R. Agarwal, and V. Lanzo, "Automated extraction of aortic and pulmonary components of the second heart sound for the estimation of pulmonary artery pressure.," *Conf. Proc. IEEE Eng. Med. Biol. Soc.*, vol. 2, pp. 921–924, 2004.
- [7] Z. Syed, D. Leeds, D. Curtis, F. Nesta, R. a. Levine, and J. Guttag, "A framework for the analysis of acoustical cardiac signals," *IEEE Trans. Biomed. Eng.*, vol. 54, no. 4, pp. 651–662, 2007.
- [8] P. Bentley, G. Nordehn, M. Coimbra, S. Mannor, and R. Getz, "Classifying Heart Sounds Challenge."
<http://www.peterjbentley.com/heartchallenge/#downloads>.
- [9] Y. Wapcaplet, "Diagram of the human heart," 2003. [Online]. Available: [http://commons.wikimedia.org/wiki/File:Diagram_of_the_human_heart_\(cropped\).svg](http://commons.wikimedia.org/wiki/File:Diagram_of_the_human_heart_(cropped).svg).
- [10] Zhao Xiu-min and Cao Gui-tao, "A novel de-noising method for heart sound signal using improved thresholding function in wavelet domain," in *2009 International Conference on Future BioMedical Information Engineering (FBIE)*, 2009, pp. 65–68.
- [11] D. L. Donoho, "De-noising by soft-thresholding," *IEEE Trans. Inf. Theory*, vol. 41, no. 3, pp. 613–627, 1995.

- [12] A. Zaeemzadeh, Z. Nafar, and S.-K. Setarehdan, "Heart sound segmentation based on recurrence time statistics," in *2013 20th Iranian Conference on Biomedical Engineering (ICBME)*, 2013, no. Icbme, pp. 215–218.
- [13] T.-H. Hung, C.-C. Chou, W.-C. Fang, A. H.-T. Li, Y.-C. Chang, B.-K. Hwang, and Y.-W. Shau, "Time-frequency analysis of heart sound signals based on Hilbert-Huang Transformation," in *2012 IEEE 16th International Symposium on Consumer Electronics*, 2012, pp. 1–3.
- [14] C. Cortes and V. Vapnik, "Support-vector networks," *Mach. Learn.*, vol. 20, no. 3, pp. 273–297, 1995.
- [15] M. Singh and A. Cheema, "Heart Sounds Classification using Feature Extraction of Phonocardiography Signal," *Int. J. Comput. Appl.*, vol. 77, no. 4, pp. 975–8887, 2013.
- [16] R.-E. Fan, P.-H. Chen, and C.-J. Lin, "Working Set Selection Using Second Order Information for Training Support Vector Machines," *J. Mach. Learn. Res.*, vol. 6, pp. 1889–1918, 2005.
- [17] D. B. Springer, L. Tarassenko, and G. D. Clifford, "Support Vector Machine Hidden Semi-Markov Model-based Heart Sound Segmentation Time," in *Computing in Cardiology*, 2014.